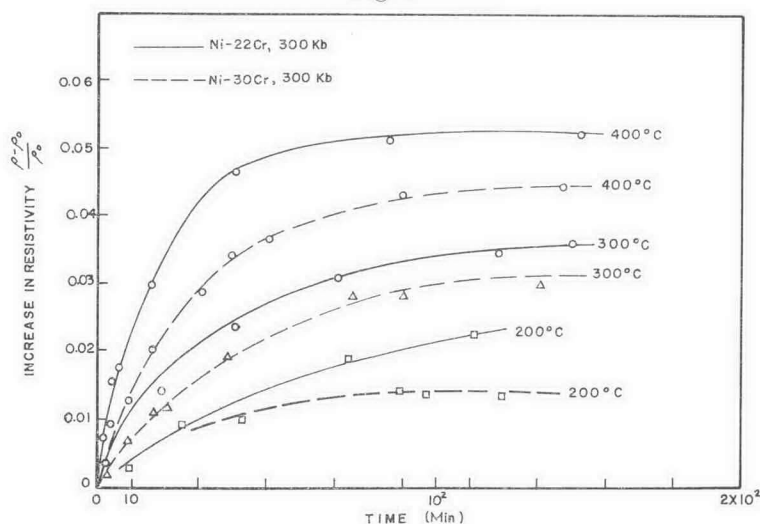


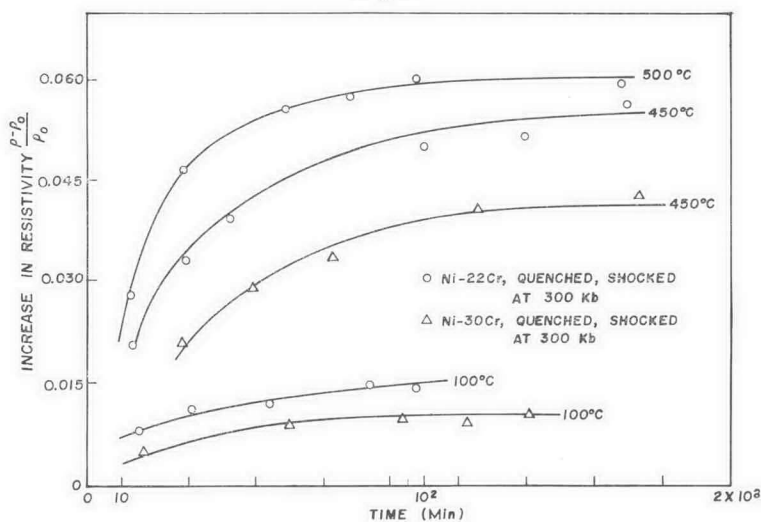
Fig. 7



Isothermal annealing of Ni-22 Cr and Ni-30 Cr after shock deformation at 300 kbar.

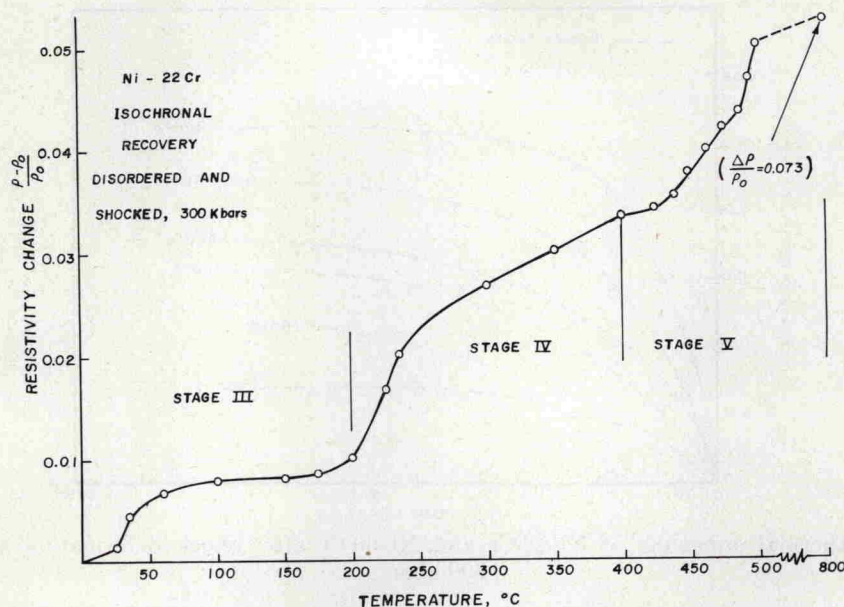
Figure 8 shows that both the Ni-22 Cr and Ni-30 Cr alloys follow a similar shaped isothermal recovery curve. Defect concentration estimates from resistivity experiments require the identification of recovery stages from isochronal annealing experiments (Christou 1972). In the present work three recovery stages were observed for Ni-22 Cr which are identified as Stages III, IV, and V (fig. 9). The specimen resistivity after shock

Fig. 8



Isothermal annealing of Ni-22 Cr and Ni-30 Cr after quenching and shock deformation at 300 kbar.

Fig. 9



Isochronal annealing of Ni-22 Cr after quenching and shock deformation at 300 kbar.

deformation is denoted as ρ_s , then $\rho_s - \rho(200^{\circ}\text{C})$ is Stage III. $\rho(200) - \rho(350)$ is Stage IV, and $\rho(250) - \rho(\text{anneal})$ is Stage V. Resistivity changes during each stage are shown in table 3. Stage V includes both the recovery of dislocations and the formation of K-state. Isochronal recovery data for the Ni-30 Cr alloys was not taken.

Table 3. Resistivity changes in stages III, IV, and V for Ni-22 Cr

P (kb)	Total strain ϵt	$\Delta\rho\text{III}$ ($\mu\Omega\text{-cm}$)	$\Delta\rho\text{IV}$ ($\mu\Omega\text{-cm}$)	$\Delta\rho\text{V}$ ($\mu\Omega\text{-cm}$)
90	0.015	0.52×10^{-2}	0.50×10^{-2}	1.20×10^{-2}
150	0.045	0.45×10^{-2}	0.40×10^{-2}	1.50×10^{-2}
300	0.070	0.42×10^{-2}	0.25×10^{-2}	1.70×10^{-2}
500	0.097	0.30×10^{-2}	0.20×10^{-2}	1.95×10^{-2}

§ 4. DISCUSSION AND CONCLUSIONS

4.1. Discussion of the Quenching Results

The quench-anneal results described in the previous section have clearly identified three types of resistivity changes. Change 1 pertains to the decrease in resistivity during non-equilibrium cooling. Change 2 is the increase in resistivity during annealing after non-equilibrium cooling.